Microscopically-viewed Structural Changes in Solvent-induced Phase Transitions of Synthetic Polymers

Kohji Tashiro, Akiko Yoshioka, Tomoko Hashida*

Department of Macromolecular Science, Graduate School of Science, Osaka University, Toyonaka, Osaka 560-0043, Japan
E-mail: ktashiro@chem.sci.osaka-u.ac.jp

Summary: Structural changes occurring in the solvent-induced phase transition have been investigated by carrying out the time-resolved measurements of X-ray diffraction, infrared spectra and Raman spectra. First example is about the solvent-induced crystallization of *syndiotactic* polystyrene glass. By comparing the time evolution of the various infrared and Raman bands and the X-ray reflections, the process of nucleation, growth, and aggregation of regular helical sequences in the crystalline lattice could be traced concretely. It was also found experimentally that the amorphous chain segments started an active motion immediately after absorbing solvent molecules and became a trigger to induce the local regularization of random coils into regular helical segments. The second example is the reversible solid-state phase transition of poly(ethylene imine) between the anhydrate of doubly-stranded helices and the hydrates of planar zigzag chains. By carrying out the time-resolved infrared spectral measurements in water vapor atmosphere (H_2O or D_2O), the characteristic bands could be identified for these crystalline phases and the structural transformation in the hydration process could be clarified in detail.

Keywords: infrared spectra; poly(ethylene imine); Raman spectra; solvent-induced crystallization; solvent-induced phase transition; syndiotactic polystyrene

Introduction

Some crystalline polymers show interesting interactions with solvent in the solid state and form various kinds of polymer-solvent complex. For example, the amorphous sample of syndiotactic polystyrene (SPS) crystallizes by absorbing such organic solvent as toluene, benzene, chloroform, etc. (Many references are listed in papers[1,2]). The molecular chain changes into -$(TTGG)_2$- helix and forms a complex with solvent molecules in the crystal lattice. This ordering process occurs at room temperature, much lower than the glass transition point of this polymer. The SPS-solvent complex changes into other crystal phases by heating, just when the solvent molecules evaporate from the sample and the molecular conformation changes from TTGG

 DOI: 10.1002/masy.200351302

form to all-trans form. What is the microscopic mechanism of these complicated phase transitions ?

Another example is about the phase transition of poly(ethylene imine) (-CH_2CH_2NH-, PEI). This polymer forms a doubly-stranded helix of -$(TTG)_n$- conformation with intramolecular hydrogen bonds.[3-5] By absorbing water molecules, the double helix changes into a pair of planar-zigzag chains, which are connected with water molecules through intermolecular hydrogen bonds. By increasing the relative amount of absorbed water molecules, the hydrate changes its structure stepwisely and stoichiometrically from hemihydrate (EI unit/water ratio = 1/0.5) to sesquihydrate (1/1.5) and to dihydrate (1/2). These transitions occur reversibly in the solid state. In order to reveal the essential features of the transition mechanism, the structural change must be clarified in detail from the molecular level.

In this paper we will describe the structural changes occurring in the crystallization and phase transition of SPS-solvent system and in the solid-state phase transition of PEI-water system through the time-resolved measurements of X-ray diffraction, infrared spectra and Raman spectra.

Crystallization and Phase Transition of SPS

Solvent-induced Crystallization of SPS Glass

SPS glassy sample was prepared by quenching the melt into ice-water bath. The sample was set in an optical cell, into which an organic solvent was injected by a syringe and the cell space was filled with solvent vapor. Figure 1 shows the time dependence of Raman spectra taken under the atmosphere of toluene vapor at room temperature. In parallel to the increment of toluene band intensity, the amorphous band (406 cm^{-1} *e.g.*) decreased in intensity and the crystalline bands characteristic of T_2G_2 helical chain conformation increased in intensity. The integrated intensity was evaluated for these characteristic bands after curve separation. Some of crystalline bands were found to appear at first immediately after the injection of organic solvent but some other crystalline bands were observed in much later timing. This phenomenon could be detected similarly in the infrared spectra. This detection time difference among the various bands is considered to come from a difference in sensitivity of a Raman or infrared band to the effective helical chain length or a difference in critical sequence length.[6] That is to say, a

crystalline band can be detected for the first time when the length of a regular helical segment is beyond a critical sequence length. By measuring the infrared and Raman bands for a series of random copolymers of hydrogeneous and deuterated styrene monomeric units, the critical sequential length could be evaluated for various bands.[1] For example, Figure 2 shows the time dependence of the relative intensity of the Raman bands with the thus-clarified critical sequence lengths. The band at 1252 cm^{-1} has a relatively short critical sequence length of ca. 10 monomeric units (ca. 2.5 helical turns) and was detected in a short time after injection of toluene. The 422 cm^{-1} band having longer critical sequence length of ca. 20 monomeric units (ca. 5 helical turns) was detected much later than that, indicating a growth of helix.

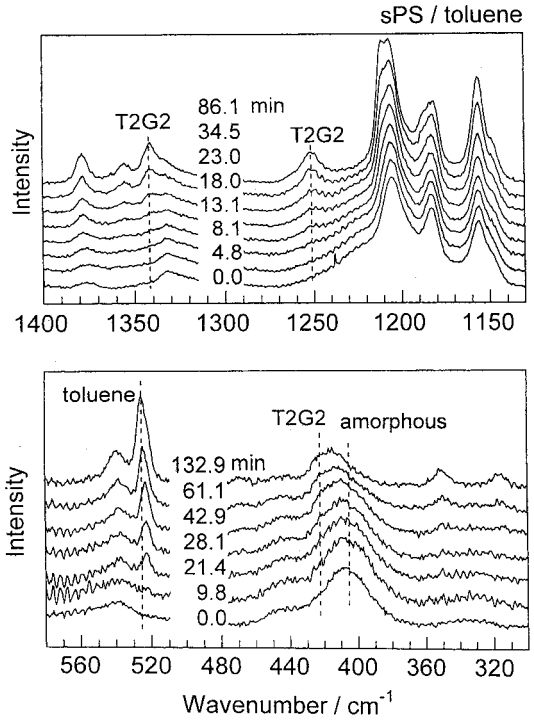

Fig. 1. Time dependence of Raman spectra measured for SPS glass during exposure to toluene atmosphere.[1]

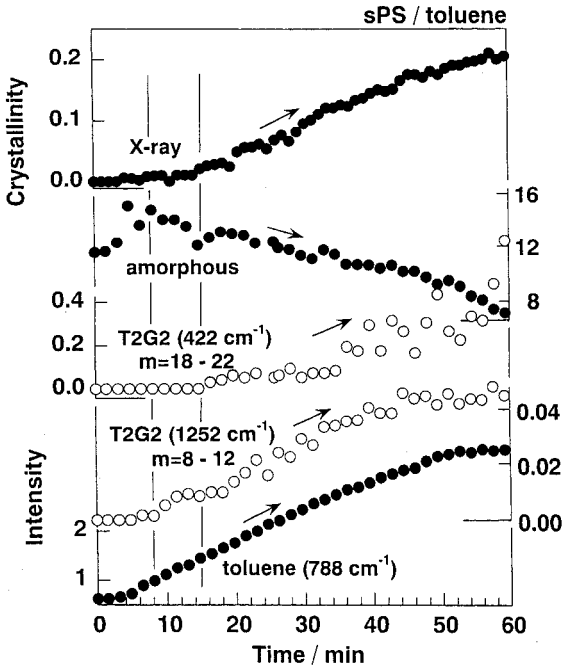

Fig. 2. Time dependence of integrated intensity evaluated for various Raman bands with different critical sequence length *m* and that of the X-ray reflection measured for SPS glass during exposure to toluene atmosphere.[1]

In parallel to this spectroscopic study, the time-resolved measurement of X-ray diffraction was made during exposure of the sample into a toluene gas. Since the thickness of the sample was essentially the same with that used in the Raman measurement, we could compare the time-evolution of the X-ray diffraction intensity with the Raman data, as seen in Figure 2. The timing to detect the X-ray diffraction intensity was almost the same with that of the first observation of Raman bands with long critical sequence length. Therefore we may speculate that the random coils in the amorphous phase change at first into regular but short helical segments, which grow into longer helical sequences and gather together to form a crystalline lattice as being observed in the X-ray diffraction.

As stated in the introduction, this solvent–induced crystallization of SPS was observed at room

temperature, much lower than the glass transition point (ca. 100°C). It may be easily speculated that the molecular motion in the amorphous phase is activated by a plasticizer effect of absorbed toluene molecules. This speculation must be proved by experiment. In order to detect the molecular motion, we utilized the half-width of an infrared amorphous band on the basis of such an idea that the band width is inversely proportional to the relaxation time in general. In fact, as seen in Figure 3, the half-width of the amorphous band at 565 cm^{-1} became wider after injection of solvent and the band position shifted to lower frequency side, indicating a start of molecular motion. Then, around 2 min, the crystalline bands with short critical sequence length began to appear. With a passage of time, the helical chain segments grew longer and formed a crystal lattice as mentioned above, just when the half-width of the amorphous band became narrower again. This may come from such a situation that the amorphous region was sandwiched between the crystalline lamellae and its motion was confined more or less due to a geometrical constraint. Figure 4 shows a concrete image of the solvent-induced crystallization phenomenon of SPS.

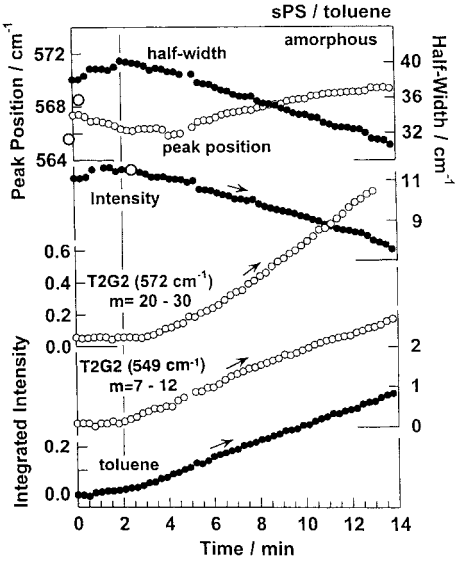

Fig. 3. Time dependence of integrated intensity of the various crystalline infrared bands with different critical sequence length *m* and the half-width and wavenumber of the amorphous band evaluated for SPS glass during exposure to toluene atmosphere.

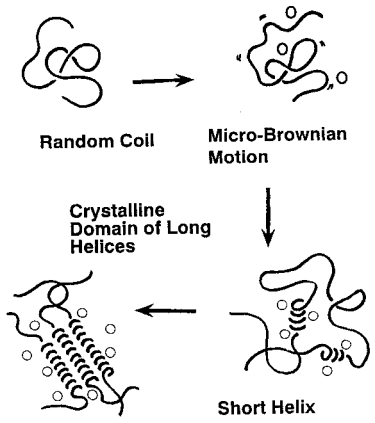

Fig. 4. A schematic illustration of ordering process of SPS random coils to the crystalline lattice of regular helical chains during the exposure to organic solvent atmosphere.

The solvent-induced crystallization of SPS glass could be detected for many kinds of solvent. As seen in Figure 5, the induction period before crystallization was longer in the order of chloroform < benzene < toluene < acetone. The crystallization rate or the slope of curve was higher in the order of chloroform >> benzene ≈ acetone > toluene. Roughly speaking, these differences in induction period and crystallization rate seem to reflect the difference in solubility (chloroform > benzene > toluene > acetone) or the difference in interaction between polymer and solvent molecule, which affects the diffusion rate of solvent into polymer matrix, the enhancement of chain motion in the amorphous region, and so on. At the same time we need to consider the size effect of solvent molecule. The effective volume is in the following order: acetone (54 $Å^3$) < chloroform (61 $Å^3$) < benzene (73 $Å^3$) < toluene (86 $Å^3$). Such a large molecule as toluene is difficult to diffuse in the amorphous matrix, resulting in longer induction period as seen in Figure 5. Smaller molecule is considered to enter the matrix relatively easily. Acetone is small in size but the solubility of SPS is low, resulting in the long induction period. Therefore the solvent-induced crystallization may be governed by a multiple effect of the solubility and molecular size of solvent.

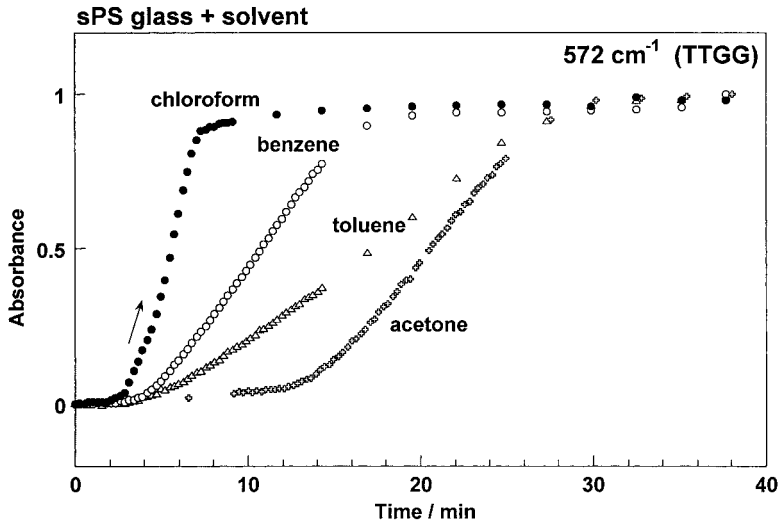

Fig. 5. Time dependence of infrared absorbance estimated for the 572 cm^{-1} T_2G_2 band in the solvent-induced crystallization proccess of SPS during exposure to various kinds of solvent atmosphere.

As for the size effect, we observed the following phenomenon. Figure 6 shows the solvent exchange phenomenon, which occurred by injecting a different kind of solvent B into the cell containing the sample of polymer-solvent A complex. The infrared band intensity of solvent A decreased immediately after the solvent B was injected to the cell, and the solvent B band increased in intensity at the same time. That is to say, the solvent A molecules captured in the holes of the complex are purged and replaced by solvent molecules B. The exchange rate was almost the same for any pair of solvents A and B, suggesting a smooth movement of the solvent molecules in the crystal lattice irrespective of the difference in relative size of the molecules. The penetration of solvent molecules into a crystal lattice is difficult in general. But it is quite easy in the SPS complex, which has already holes to trap the solvent molecules. When the crystal structure of δ form is viewed along the chain axis, as shown in Figure 7, it is noticed that the guest solvents are packed in a columnar form along the chain axis.[7] As a possibility, we may speculate that the external solvent B approaches the surface of δ-form crystallite and

affects the whole system. Then the neighboring T_2G_2 chain stems are forced to move slightly because of swelling effect and the radius of solvent column is expanded to some extent just like an opening of gate. Then solvent B can migrate into the tunnel smoothly and solvent A goes out of the column instead. After that the complex between the polymer stems and solvent B is energetically stabilized and the gate is closed again. Another possible way of opening the gate is a cooperative reorientation of phenylene side groups of chain stems, which may make the hole wider at a moment and allows the solvent molecules B to enter the holes smoothly. Anyway, an easy exchange of solvents at almost common rate (Figure 6) is considered to reflect such a situation that the interaction between polymer and solvent is very weak and SPS polymers are difficult to recognize the difference of solvent molecules. Of course, as known from the

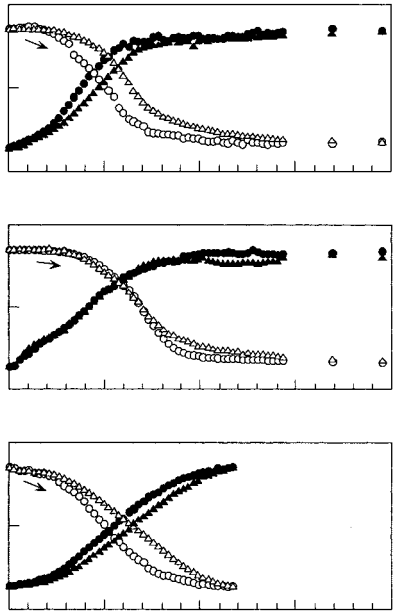

Fig. 6. Time dependence of infrared absorbance of solvent bands during the solvent exchange process. For example, in the top figure, the exchange occurs from benzene or toluene to chloroform by injection of chloroform into the SPS complex with the corresponding solvent.

observation that the infrared bands of absorbed solvent appear at slightly different frequency positions from those of pure liquid state for most of the cases, the interaction between polymer chains and solvent molecules can not be ignored perfectly. But this frequency shift is only several wavenmubers. The spectral pattern of the absorbed solvent is rather similar to that of pure liquid, although the half-width is a little narrower in the former case. This suggests that the solvent molecules in the complex may behave like those in the liquid state but with some limited thermal motion in the lattice.

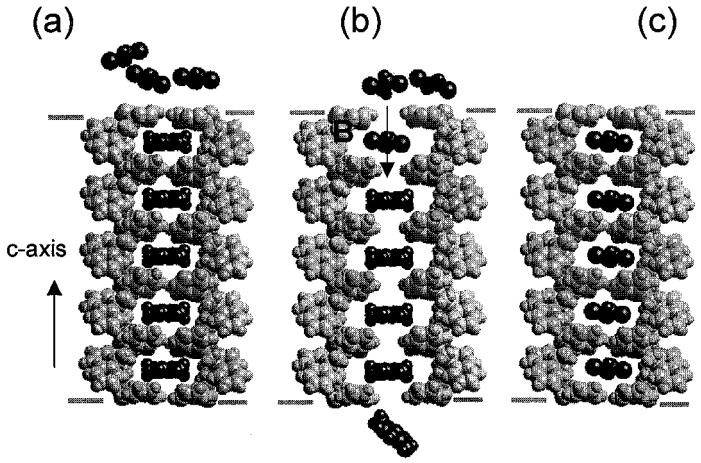

Fig. 7. A schematic illustration of one possible solvent-exchange process.Solvent A forms a column in parallel to the chain axis. (a) solvent A is trapped in between the extended chain stems of T_2G_2 form. The solvent B approaches the crystallite. (b) The interchain distance is increased, just like a swelling phenomenon. As a result, the free space becomes larger and the solvent A is displaced by solvent B. (c) The interchain distance is contracted again to attain the energetically-stable structure of SPS-solvent B complex.

Thermally-induced Phase Transition of SPS

By heating the δ form in the air atmosphere, the solvent molecules are evaporated and the δ form changes into the γ form, which has the same T_2G_2 conformation but does not contain solvent anymore. This γ form changes into the α form of planar-zigzag conformation by heating above 185°C. The infrared spectra were measured during these phase transitions and the relative intensity of various infrared bands is plotted against temperature as shown in Figure 8, where

the case of toluene is presented. The infrared bands intrinsic of toluene (730 cm^{-1}) and δ form (780 cm^{-1}) gradually decreased in intensity from the start of heating. At the same time the bands of γ form (776 cm^{-1}) began to appear and increased in intensity. At about 140°C, this transition ceased perfectly. The thus-generated γ form was kept for a while, and then decreased steeply in a narrow temperature region of about 190°C and the α form increased at the same time. At higher temperature the infrared bands of α form disappeared and the sample was melted. When the solvent was changed to benzene or chloroform, the evaporation rate of solvent was different among them, but infrared bands of solvent and δ form disappeared at ca. 140°C, almost commonly to the case of toluene. As discussed before, the polymer-solvent interaction is weak and the solvent evaporation occurs at almost the same rate as suggested from the solvent exchange phenomenon (Figure 6). Similar transition temperature among the various solvents may originate from such a situation. Ramesh et al. reported more detailed experimental data, saying that the transition temperature from δ to γ form was not related with the kind of solvent used in the experiment but was determined almost only by the relative content of absorbed solvent.[8]

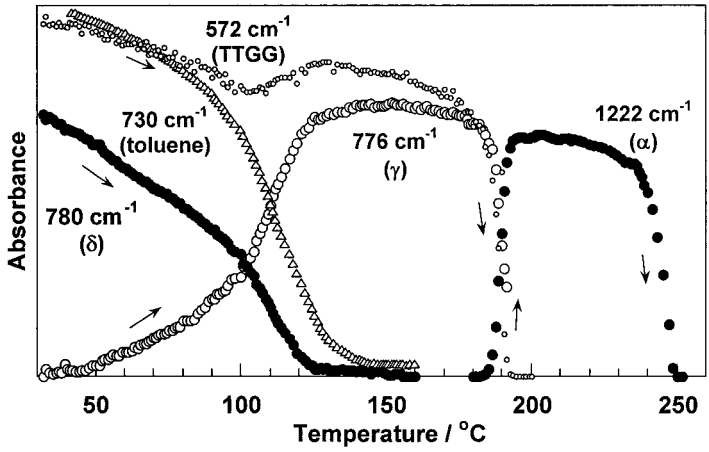

Fig. 8. Temperature dependence of integrated intensity of the infrared bands characteristic of various crystalline forms in the heating process from the δ form containing tolene solvent.

Hydration-Induced Phase Transition of Poly(ethylene imine)

As already stated in the introductory session, poly(ethylene imine) (PEI) takes a doubly-stranded helix of -$(TTG)_n$- conformation in the dry state. When water is supplied, the anhydrate changes into the hydrate of planar-zigzag chains. The hydrates exist in three types, depending on the relative content of ethylene imine (EI) and water; hemihydrate (EI/water = 1/0.5), sesquihydrate (1/1.5) and dihydrate (1/2).[3–5] By measuring the infrared spectral changes during hydration process, the transition behavior was investigated in detail.[9] Figure 9 (a) shows the time dependence of the infrared spectra during hydration process. By absorbing water, the infrared bands of the anhydrate (800 cm^{-1}) decreased in intensity and the other new bands (876 and 918 cm^{-1}) started to appear and increased in intensity. But the detailed intensity changes of these bands could not be estimated exactly because of an overlap of broad water bands. Then, the water to be injected into the cell was changed from light water (H_2O) to heavy water (D_2O) with expecting a lower frequency shift of the broad bands of H_2O. As shown in Figure 9 (b), the intensity exchange between the various bands of hydrates could be observed more clearly by using heavy water. By estimating the intensity of the infrared bands intrinsic of various crystal modifications, the phase transition from anhydrate to hemihydrate, sesquihydrate and to dihydrate could be traced definitely. When the spectral changes were investigated in more detail, it was found that the amorphous bands decreased in intensity in parallel to the phase transition from anhydrate to hydrates. That is to say, when the PEI anhydrate absorbs water, not only the anhydrate crystalline phase but also the amorphous phase changes into the hydrates as illustrated in Figure 10. If this ordering process in the amorphous phase occurs ideally and perfectly over the whole sample, then the hydrate with 100% crystallinity should be obtained at the final stage of hydration. But it could not occur perfectly because of the existence of chain entanglements which may disturb the regularization of random coils. The situation is very similar to the above-mentioned SPS case, in which the degree of crystallinity does not reach 100 % even when the absorption of organic solvent is saturated.

When the anhydrate sample was heated up, it melted around 60°C in the dry state. When the anhydrate sample containing slight amount of water was heated, the water molecules in the amorphous region migrated and entered the crystalline phase, causing a transition of anhydrate to hydrate at such a low temperature as 40°C. The thus created hydrates melted at about 80°C

and then the water molecules went away into the amorphous region. When the sample contained larger amount of water, the dihydrate phase was overwhelming in the sample. This phase was found to change to sesqui- and hemihydrates by heating up to ca. 60°C, and these hydrates melted at about 70°C. This observation indicates that the dihydrate has weaker hydrogen bonds with water and transfers easily to hemi- or sesquihydrate by releasing water molecules on heating. In this way, depending on the relative content of water, the crystalline phases in the starting sample and their phase transition behaviors are changed sensitively and in a complicated manner.

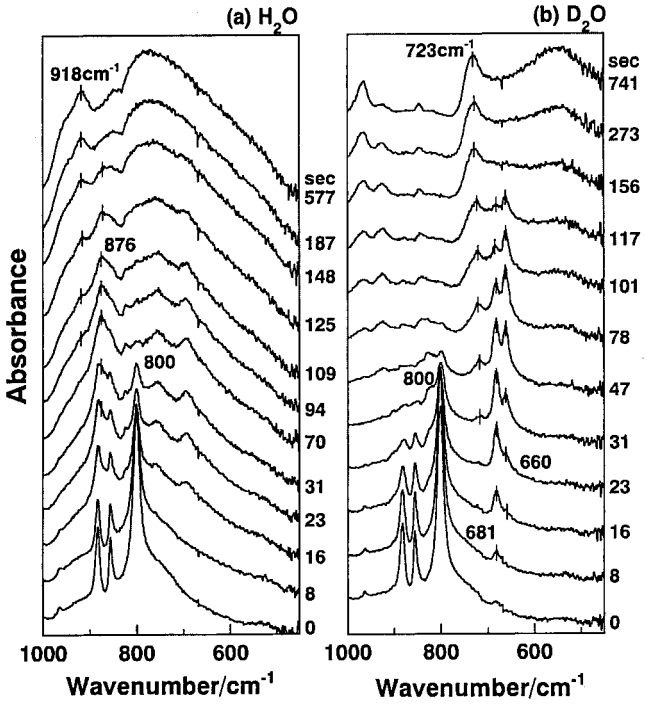

Fig. 9. Time dependence of infrared spectra of PEI exposed to water vapor atmosphere at room temperature. (a) H_2O and (b) D_2O.[9]

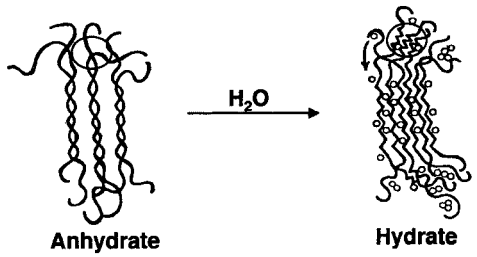

Fig. 10. An illustration of structural change in the hydration-induced phase transition of PEI from anhydrate of doubly-stranded chains to hydrate of planar-zigzag chains. Not only the crystalline phase but also the amorphous phase changes the structure partly.

Acknowledgements

The authors wish to thank Idemitsu Petrochemical Co., Ltd., Japan for supplying SPS samples. They also thank Drs. Yoshiaki Inaki and Sadahito Aoshima of Osaka University for their kind discussion in the PEI study.

[1] K. Tashiro, Y. Ueno, A. Yoshioka, M. Kobayashi, *Macromolecules* **2001**, *34*, 310.
[2] K. Tashiro, A. Yoshioka, *Macromolecules* **2002**, *35*, 410.
[3] Y. Chatani, H. Tadokoro, T. Saegusa, H. Ikeda, *Macromolecules* **1981**, *14*, 315.
[4] Y. Chatani, T. Kobatake, H. Tadokoro, R. Tanaka, *Macromolecules* **1982**, *15*, 170.
[5] Y. Chatani, T. Kobatake, H. Tadokoro, *Macromolecules* **1983**, *16*, 199.
[6] M. Kobayashi, K. Akita, H. Tadokoro, *Makromol. Chem.* **1968**, *118*, 324.
[7] Y. Chatani, Y. Shimane, T. Inagaki, T. Ijitsu, T. Yukinari, H. Shikuma, *Polymer* **1993**, *34*, 1620.
[8] E. Bhoje Gowd, Smitha S. Nair, C. Ramesh, *Macromolecules*, in press.
[9] T. Hashida, K. Tashiro, S. Aoshima, Y. Inaki, *Macromolecules* **2002**, *35*, 4330.